SeaWinds on QuikScat Radiometric Measurements and Calibration

W. Linwood Jones, Rushad Mehershahi, and Josko Zec
Central Florida Remote Sensing Laboratory
UCF - Electrical and Computer Engineering Dept.
PO Box 162450
Orlando, FL 32816-2450, USA
Voice (407) 823-6603; fax 823-5835
ljones@pegasus.cc.ucf.edu

David G. Long
Microwave Earth Remote Sensing Laboratory
BYU Center for Remote Sensing
BYU Department of Electrical and Computer Engineering
459 Clyde Building
Provo, Utah 84602

I INTRODUCTION

Originally designed as a radar scatterometer [1], SeaWinds measurements have recently been expanded to include brightness temperature of the earth. Not since 1972, when the S-193 RADSCAT flew on NASA's SkyLab, has such a combined active/passive microwave remote sensor in flown in space. Now, with the launch of the SeaWinds on the QuikScat satellite in June of 1999, simultaneous, active/passive measurements are again available for earth remote sensing. This technological advance is the result of several changes in the SeaWinds instrument configuration compared to previous satellite scatterometers (SeaSat, ERS-1 & -2 and NSCAT). Foremost, SeaWinds uses conical scanning "pencil" beams to simultaneously measure both the surface backscatter and microwave emission. In this paper we describe the radiometric processing and calibration that enables the surface brightness temperature measurement.

II RADIOMETRIC MEASUREMENT

Instrument Transfer Function

The SeaWinds instrument is a 13.4 GHz radar scatterometer with a mechanical spinning reflector antenna (Fig. 1). The backscattered energy is collected over the entire conical scan

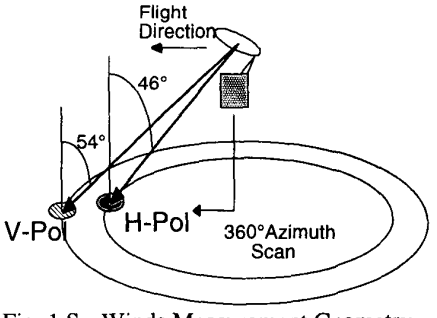

Fig. 1 SeaWinds Measurement Geometry

This work is sponsored by NASA Headquarters through the Jet Propulsion Laboratory's QuikScat Project.

(forward and aft looking) with separate offset pencil beams, vertical or horizontal polarization. The pulse repetition frequency and antenna scan rate have been designed to provide approximately 50% overlap of the instantaneous field of view (IFOV) in both the along track and cross track directions. The radiometric function is a recent addition that is implemented through signal processing. Thus with the pencil beams, it is possible to isolate the "graybody" microwave emissions from the earth into elliptical footprints defined by the one-way antenna pattern half-power contours (approximately 35 km x 50 km).

The simplified instrument block diagram for receiving is given in Fig. 2. For the radar measurement, the received signal plus noise is measured simultaneously in two overlapping channels; a narrow-band "echo" channel (250 KHz) and a wider-band "noise" channel (1 MHz). The echo channel matches the backscatter spectrum and thereby captures all of the energy in the radar return echo. The noise channel captures the radar echo plus the flat energy spectrum of the antenna collected earth brightness and the internally generated receiver noise. For the scatterometer measurement, an estimate of the noise energy En is subtracted from the echo channel output energy Ee to derive the backscattered energy. For radiometric processing, we reverse the process and calculate the excess noise energy given by:

$$N_x = E_n - \beta E_e = k\,T_{sys}(B_n - B_e)G_n\tau \qquad (1)$$

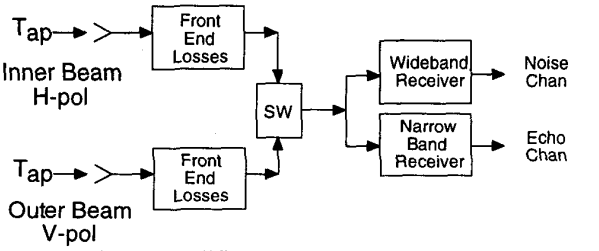

Fig. 2 Simplified Receiver Block Diagram

where $\beta = G_n/G_e$ is the gain ratio where G_n is the noise channel gain and G_e is the echo channel gain; k = Boltzman's constant, J/K; $T_{sys} = T_{ant} + T_{rec}$ is the system noise (radiometric) temperature, K; T_{ant} = is the antenna (radiometric) temperature, K; T_{sys} = is the receiver noise temperature, K; B_n = the noise chan bandwidth, Hz; B_e = the echo chan bandwidth, HZ, and τ is the range gate width (integration period).

The antenna temperature is the input to the receiver that includes both the earth's apparent brightness temperature (T_{bap}) collected by the antenna and the noise emitted transmission line losses in front of the receiver input:

$$T_{ant} = T_{bap} * FEloss + (1 - FEloss) * T_{phys} \qquad (2)$$

The effect of the front-end loss is to attenuate the brightness signal and to add a bias temperature proportional to its physical temperature T_{phys}. Thus, by accurately characterizing the SeaWinds instrument transfer function (losses, gains, and component noise figures) as a function of the operating physical temperature, then good estimates of the surface apparent brightness temperature can be made. Fortunately, pre-launch SeaWinds calibrations during thermal vacuum testing are available to estimate the transfer function parameters. Also, on-orbit measurements obtained in the receive only mode are extremely valuable in radiometric characterization in the absence of radar echo's.

Radiometric Calibration

Designed as a radar, SeaWinds is not an optimum radiometer. Brightness temperatures (T_b's) are calculated for each pulse period with an equivalent integration time of 1.5 ms. Because of the limited receiver bandwidth, the radiometric precision is larger than desired (ΔT = 27 Kelvin/pulse). This can be partially ameliorated by using spatial and temporal averaging; and to this end, QuikScat radiometer (QRad) apparent brightness temperatures are now included in the level-1B data product [2]. This results in two apparent brightness temperatures, one for each polarization or beam, for each SeaWinds 25 km wind vector cell. Both forward-looking and aft-looking azimuth directions are collocated into the final product that consists of 4 to 6 pulses averaged to produce a $\Delta T < 12$ Kelvin.

Unfortunately for QRad there are no provisions for absolute brightness calibration; however, a single-point relative radiometric calibration performed once per antenna scan whereby the receiver is terminated in an ambient temperature load. This measurement allows the average receiver gain to be measured with high precision. During six months of on-orbit testing, the instrument parameters, used in the radiometric transfer function, have demonstrated excellent stability, and this enables highly-repeatable relative T_b's to be measured. To provide an absolute calibration, an external comparison with the Tropical Rainfall Measuring Mission (TRMM) Microwave Imager (TMI) is adopted. During this procedure, 3-day average T_b's are produced for QRad on a fixed earth grid for horizontal and vertical polarizations. To collocate with TMI, the brightness measurements cover the earth from ± 35° latitude with a grid resolution of 0.25° latitude x 0.25° longitude.

For TMI, the two lowest frequency channels at 10.7 GHz and 19 GHz bracket the Qrad at 13.4 GHz; however, the incidence angles do not match. The TMI incidence angle is 52.8°for all channels; whereas, for QRad, the inner (H-pol) beam is 46° and the outer (V-pol) beam is 54°. Thus, TMI Tb's are translated into "equivalent" QRad measurements before comparisons are made. For oceans, a radiative transfer model is used to calculate the equivalent QRad brightnesses from the TMI observations. Over oceans, model results are accurate to within a few Kelvin; however, for land the situation was more complex. Because of the wide variability of the dielectric properties of terrain, it was not possible to develop an simple analytical model to calculate QRad T_b's. At vertical polarization, T_b's are measured at similar incidences (52.8° vs. 54°). Thus, TMI measurements are interpolated with a small incidence angle correction. For horizontal the seven degree difference in incidence angle requires a significant adjustment that depends upon the assumed variation of surface emissivity with incidence angle. The Amazon rain forest is a large homogeneous, isotropic region that can be modeled as a Lambertian surface with a cosine dependence on incidence angle. Thus, this and other rain forrest regions are used as the hot targets for QRad H-polarization. Finally, because the QRad/TMI T_b's are not collocated instantaneously in time, transient rain events may be present in one or the other ocean data sets that can produce significant differences (10's of Kelvin) at a given locations. This "error" is effectively removed by spatial and temporal (3-day) averaging. A plot of the linear regression curves for H- and V-pols is given in Fig. 3 and the slopes and biases are given in Table-1. These calibration results demonstrate the effectiveness of this external calibration technique.

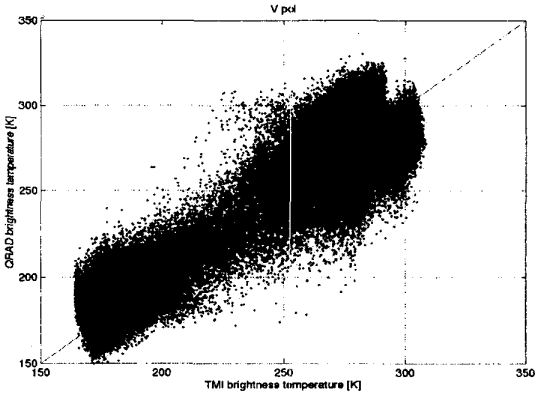

Fig. 3a Comparison of TMI and QRad H-Polarization Brightness Temperatures

Period	Slope h-pol	Offset h-pol	Slope v-pol	Offset v-pol
Aug. 99	0.98	3.97	0.94	5.25
Sept. 99	0.98	3.87	0.94	4.75
Oct. 99	0.99	2.24	0.95	0.94
Jan. 00	1.06	-1.06	1.02	-7.78
Apr. 00	1.04	1.46	1.02	-7.95

Table 1: TMI vs. QRAD linear coefficients

Radiometric Stability

The stability of the QRad T_b's are assessed by monthly 3-day comparisons and by processing the mean ocean brightness for repeating ground tracks (swaths) that occur every 41 orbits. Results from the 3-day comparisons, presented in Table-2, show excellent stability for spatial and temporal averages. The variability of the slopes and biases are small and produce changes in the absolute calibration of only a few Kelvin. Results of the repeating ground tracks are presented in Fig. 4 for passes that occur in the middle of the Pacific ocean between ± 70° latitude. This location is selected because it is far from land masses that can increase the T_b's by an unknown amount. From the envelope of the brightness temperature curves, it is obvious that the orbit to orbit stability is very good.

III CONCLUSIONS

The Qrad brightness temperatures in the SeaWinds level-1B product [2] is a reliable source of data that may be used to estimate geophysical parameters that have strong T_b's signatures or that have large spatial or temporal scales such that averages can be made to improve the measurement precision. Examples of applications that are being pursued are rain measurements over oceans and sea ice extent measurements. Most likely there will be new applications that will benefit by these combined active/passive microwave measurements.

IV REFERENCES

1. M.W. Spencer, C. Wu, D.G. Long, "Tradeoffes in the design of aspaceborne scanning pencil beam scatterometer: Application toSeaWinds," Trans. Geosci. Remote Sensing, Vol. 35, pp. 115-126, Jan. 1997.
2. SeaWinds Project Data distributed by the Jet Propulsion Laboratory Physical Oceanography Distributed Active Archive Center (PODAAC)

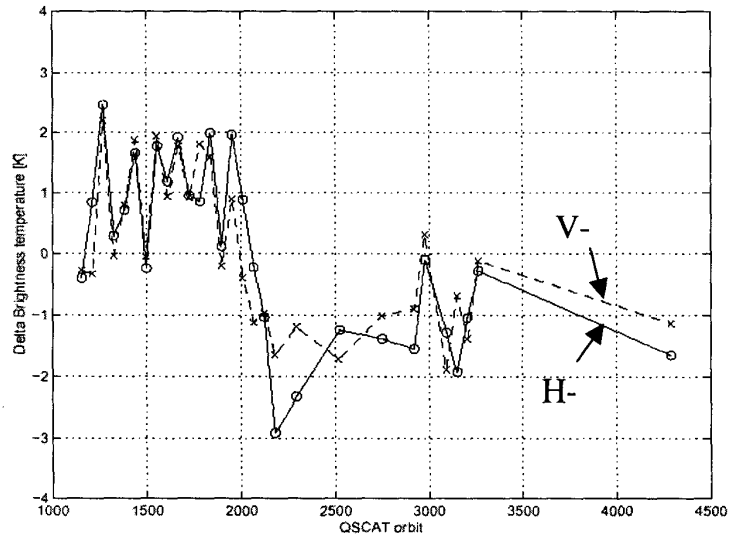

Fig. 4 Orbit Average Brightness Temperatures for Repeating Ground Track Ocean Passes